Environmental Pollution 172 (2013) 61–69

Contents lists available at SciVerse ScienceDirect

Environmental Pollution

journal homepage: www.elsevier.com/locate/envpol

Biomonitors of urban air pollution: Magnetic studies and SEM observations of corticolous foliose and microfoliose lichens and their suitability for magnetic monitoring

Marcos A.E. Chaparro [a,b,*], Juan M. Lavornia [c], Mauro A.E. Chaparro [d], Ana M. Sinito [a]

[a] *Instituto de Física Arroyo Seco (IFAS, UNCPBA)-CONICET, Pinto 399, 7000 Tandil, Argentina*
[b] *Centro de Geociencias, UNAM, Blvd. Juriquilla 3001, 76230 Juriquilla, Querétaro, Mexico*
[c] *Centro de Investigaciones y Estudios Ambientales (CINEA, UNCPBA)-CONICET, Pinto 399, 7000 Tandil, Argentina*
[d] *Instituto Multidisciplinario de Ecosistemas y Desarrollo Sustentable (UNCPBA)-CONICET, Pinto 399, B7000GHG Tandil, Argentina*

ARTICLE INFO

Article history:
Received 28 May 2012
Received in revised form
16 August 2012
Accepted 17 August 2012

Keywords:
Biomonitoring
Magnetic susceptibility
Lichen
Atmospheric pollution
Multivariate analysis

ABSTRACT

This study explored the suitability of available lichen species as air pollution biomonitors and assessed their potential for magnetic monitoring in cities. Several lichens on tree bark were collected in urban and industrial sites from Tandil city, as well as control sites. The results showed that magnetite-like minerals were the main magnetic carriers in all sites and samples. However, the concentration varied between clean and polluted sites. In addition, magnetic-grain size-distribution showed clear differences between sites. Observations by scanning electron microscopy showed different particles in a variety of shapes and grain sizes; moreover, the presence of iron oxides and several toxic elements was detected by energy dispersive spectroscopy analysis. Although eleven lichen species were identified that appeared suitable for use as air-pollution monitors, three of them, *Parmotrema pilosum*, *Punctelia hipoleucites* and *Dirinaria picta*, occurred more frequently in the area, thus constituting appropriate species for future monitoring in the study area.

1. Introduction

Organisms, such as lichens, which quantify environmental quality and whose parameters change in response to pollution are called “biomonitors”. They can be employed as “data integrators” since they are able to record the effects of environmental changes over time. One of the main effects of air pollution on biomonitors is bioaccumulation of elements (Basile et al., 2007; Cloquet et al., 2009; Guerra et al., 2011). Lichens are known to be sensitive to various pollutants and are considered a good biological indicator of air quality, and thus they are widely used in environmental studies (Hawksworth and Rose, 1970; Pfeiffer and Barclay-Estrup, 1992; Scerbo et al., 2002; Jasan et al., 2004; Carreras et al., 2005). Lichens are widespread and easy to sample, although not found everywhere. Air pollution may decrease the amount of lichens available to almost zero. The sensitivity of lichens to heavy metals is species-dependent and mainly influenced by morphological and structural features (Getty et al., 1999). Because the pollutants affect the lichen species with the most exposed surface to the atmosphere, their sensitivity varies according to the type of growth form, being higher in foliose-type and decreasing in microfoliose- and crustose-types (Seaward, 1987; Sutton et al., 2004; Hazarika et al., 2011).

Magnetic techniques, using natural surfaces as passive collectors of particulate pollution, are sensitive, rapid and relatively cheap, and they require no power source or protection from vandalism (Mitchell et al., 2010). In the field of environmental magnetism, magnetic measurements have been accepted for mapping anthropogenic heavy metal pollution (Thompson and Oldfield, 1986; Petrovský and Ellwood, 1999; Evans and Heller, 2003). A number of studies of air pollution based on the magnetic properties of vegetation samples have been carried out since the 1990s (Flanders, 1994; Matzka and Maher, 1999; Jordanova et al., 2003; Maher et al., 2008). Although different vegetation species – tree leaves, needles, tree ring cores, mosses – have been used as passive dust collectors in magnetometry, a small number of lichen samples have recently been studied (e.g. Moreno et al., 2003; Hanesch et al., 2003; Gautam et al., 2005; Lehndorff et al., 2006; Zhang et al., 2008, 2012; Jordanova et al., 2010; Fabian et al., 2011; Salo et al., 2012).

In Argentina, studies on the multi-elemental composition of the environment using bioindicators have mainly been undertaken

* Corresponding author.
E-mail address: chapator@exa.unicen.edu.ar (M.A.E. Chaparro).

0269-7491/$ – see front matter © 2012 Elsevier Ltd. All rights reserved.
http://dx.doi.org/10.1016/j.envpol.2012.08.006

using lichens (Calvelo and Liberatore, 2004; Carreras and Pignata, 2002; Pignata et al., 2004; Carreras et al., 2005; Bermudez et al., 2009). Epiphytic plants are efficient air pollution biomonitors because they obtain their nutrients from the atmosphere and have no contact with the soil (Wannaz et al., 2006). Studies of lichens on rock have been carried out by Lavornia (2009), and these showed that richness and diversity in the saxicolous lichen communities decrease according to proximity to the city (Tandil).

The present work focuses on the study of lichen species and their relationship with pollutants released by urban and industrial activities. In particular, such epiphytic species are passive collectors that incorporate atmospheric pollutants into their diamagnetic matrix over long periods (years). This fact, and the natural and strategic distribution in some cities, may indicate them to be useful tools as environmental controls. Indigenous lichens living on tree bark were collected in urban and control sites, and their magnetic properties were measured and compared. In addition, the suitability of different species as magnetic biomonitors in this urban area was evaluated.

2. Methods and sampling

2.1. Sampling

Sampling campaigns were carried out in Tandil city, in urban, industrial and control (unpolluted or clean) sites (Table 1, Fig. 1). Tandil is located in the Buenos Aires province (37° 19.5′S; 59° 08.3′W, Argentina) near the Tandilia belt. It is a relatively small city (~120,000 inhabitants) with few factories (about 0.2 per km^2) located in the urban area, where the pollution problem is recent and is not of long-range (Chaparro et al., 2002).

A total of 29 samples of different lichens on tree bark were collected at 20 sites according to species availability. The coordinates of sites were recorded using a Garmin GPS-system. A minimum collection height of 1.5 m was used to avoid, as much as possible, the influence of soil particles. The samples were not washed in order to investigate pollutants deposited and incorporated into this epiphytic organism. Samples were carefully collected using plastic scrapers and tools to avoid contamination. At most sampling sites, enough material (10–35 g) was collected in dry weather periods to obtain representative subsamples for magnetic and additional studies.

2.2. Lichen identification

Lichen species were identified in the laboratory of CINEA using local keys of lichen (Adler, 1992; Scutari, 1992), techniques of chemical analysis of substances (colour spot test) and by analysis of morphological and anatomical characters using a stereoscope and microscope.

2.3. Magnetic measurements

Biological material was placed and packed into standard plastic containers (~11.5 cm^3) and weighed (up to 4 g) for magnetic measurements. The rock-magnetic measurements were carried out in the laboratory of IFAS (Tandil, Argentina).

Measurements of magnetic susceptibility were made using the magnetic susceptibility meter MS2 (Bartington Instruments Ltd.) Linked to the MS2B dual-frequency sensor (0.47 and 4.7 kHz). The volumetric susceptibility (κ), κ_{FD}% frequency-dependence ($\kappa_{FD}\% = 100 \times [\kappa_{0.47} - \kappa_{4.7}]/\kappa_{0.47}$) and mass-specific susceptibility (χ) were computed.

The anhysteretic remanent magnetisation (ARM) was imparted using a partial ARM (parm) device attached to a shielded demagnetiser (Molspin Ltd.). The remanent magnetization was measured with a spinner fluxgate magnetometer (Minispin, Molspin Ltd.). Anhysteretic susceptibility (κ_{ARM}) was estimated using linear regression for ARM acquired at different DC bias fields (7.96, 47.75 and 71.58 A/m) and an alternating field (AF) of 100 mt. The κ_{ARM}/κ-ratio and the King's plot (κ_{ARM} versus κ, King et al., 1982) were also studied.

The isothermal remanent magnetisation acquisition (IRM) studies were performed using a pulse magnetiser model IM-10-30 (ASC Scientific). Each sample was magnetised by exposing it to growing stepwise DC fields, from 4.3 mt to 2470 mt. The remanent magnetisation after each step was measured using the above-mentioned magnetometer Minispin. In these measurements, IRM acquisition curves and the saturation of IRM (SIRM = IRM_{2470mt}) were determined using forward DC fields. Remanent coercivity (H_{cr}), S-ratio (=$-IRM_{-300mt}$/SIRM), ARM/SIRM and SIRM/κ ratio were also calculated.

2.4. Microscopy and elemental studies

Selected lichen samples, without any magnetic extraction, were examined by scanning electron microscopy (SEM), using a JEOL JSM-6460LV microscope. Before SEM observation, each specimen was prepared with a thin coating of Au/Pd. The composition was analysed by X-ray energy dispersive spectroscopy (EDS) investigations. The system used was an EDAX Genesis XM4 – Sys 60, equipped with Multichannel Analyser EDAX mod EDAM IV, Sapphire Si(Li) detector and Be Super Ultra-Thin Window running EDAX Genesis version 5.11 software.

2.5. Multivariate analyses

Multivariate statistical analyses, principal coordinate analysis (PCoordA) and *K*-means cluster analysis (CA), were performed using the software infostat (infostat, 2009).

One of the aims of PCoordA (Gower, 1966, 1987) is to achieve a graphic representation of D ($Dn \times n$), which is a distance matrix (distance between individuals or cases) and where n is the number of analysis units. In this study, the Gower's distance (d_G, see Chaparro et al., 2008) was used as a dissimilarity measure for the PCoordA. The PCoordA allows the identification of similarities between cases, and in consequence it is possible to investigate the existence of grouping, i.e. Groups of analysis units with a homogeneous behaviour.

The CA is a simple way to examine similarities and dissimilarities of a given data set. The *K*-means clustering partitions the objects into *K* clusters, which are defined a priori; these objects within each cluster are as close to each other, and as far from objects in other clusters, as possible. A measure of validation of clustering is the within-cluster sum of squares by cluster; the lowest value indicates the best clustering.

Detailed information and the usefulness of these multivariate statistical methods for environmental magnetism can be found in Chaparro et al. (2008, 2012).

3. Results and discussion

3.1. Lichen species

Lichens were identified and classified in the laboratory: they involved two type of growth form (foliose and microfoliose), 11 species, eight genus, and three families, including *Parmotrema pilosum*, *Punctelia hipoleucites*, *Punctelia subpraesignis*, *Teloschistes chrysophthalmus*, *Hyperphyscia aff coraloidea*, *Flavorparmelia soredians*, *Dirinaria picta* and *Dirinaria applanata*. Among them (see Table 1), *P. Pilosum* ($n = 13$), *Punctelia* spp. (i.e. *P. Hipoleucites* and *P. Subpraesignis*, $n = 8$) and *Dirinaria* spp. (i.e. *D. Picta* and *D. Applanata*, $n = 5$) were the most available in the study area.

Although the study area comprises mainly sampling sites in the urban area, it was possible to observe a decrease of proportion of foliose species from sites in the complementary area (Table 1) towards more urbanised and industrial sites. Three out of four species found in control sites were foliose, while in the complementary area (near factories or streets, traffic moderate or high) three foliose and two microfoliose were found. The factories showed a major proportion of tolerant growth types, where three out of the four species found were the microfoliose type.

It is worth mentioning the advantages of lichen species living on a vegetal substratum (tree bark) for air pollution monitoring in cities. These passive collectors are, generally, well-distributed in urban areas allowing an effective mapping at low cost where other natural collectors (leaves or urban soils) may be unsuitable or non-available.

3.2. Magnetic properties

Magnetic measurements and parameters are shown in Table 1 and Figs. 2–5, 7 and 8. The IRM studies and parameters *S*-ratio (0.88–0.98) revealed the predominance of ferrimagnetic mineral for all samples. From the IRM studies (Fig. 2), it is noted that most of the samples reach the SIRM, or ~95% of the saturation, at 300 mt as is expected for a magnetite population. A predominant magnetic phase was observed from these results, which was reproducible for most of the samples and was characterised by well-defined values

Table 1
Sampling sites and classification of collected lichen (on tree bark, $n = 29$). Magnetic properties related to concentration and mineralogy are listed. Results from multivariate analysis, *K*-means clustering partitions, are also listed.

Sample	Site [latitude; longitude]	Site obs.	Species	Growth form	χ [10^{-8} m^3/kg]	ARM [10^{-6} A m^2/kg]	SIRM [10^{-3} A m^2/kg]	κ_{ARM}/κ [dimensionless]	κ_{FD} [%]	ARM/SIRM [dimensionless]	SIRM/κ [ka/m]	H_{cr} [mt]	*S*-ratio [dimensionless]
Ca-1	37° 19.337′S; 59° 4.998′W	Campus (~2.4 km from a factory)	*Parmotrema pilosum*	Foliose	86.2	539.1	13.6	8.9	3.0	0.040	15.8	35.6	0.916
RU-1	37° 19.274′S; 59° 6.121′W	National route	*Punctelia hypoleucites*	Foliose	99.6	424.0	14.8	6.0	2.7	0.029	14.9	35.8	0.964
DO-1	37° 20.231′S; 59° 8.434′W	Street, low traffic	*Parmotrema pilosum*	Foliose	70.0	294.2	10.4	5.9	1.8	0.028	14.8	37.5	0.968
Fa-1b	37° 19.410′S; 59° 6.629′W	Factory, street, high traffic	*Dirinaria picta*	Microfoliose	134.7	450.4	19.1	4.7	0.8	0.024	14.2	38.6	0.959
Fa-2b	37° 19.376′S; 59° 6.580′W	Factory, street, high traffic	*Parmotrema pilosum*	Foliose	179.9	465.3	23.9	3.7	2.0	0.019	13.3	34.6	0.970
Fa-3b	37° 19.321′S;	Factory, street,	*Parmotrema pilosum*	Foliose	123.3	401.9	17.4	4.6	0.2	0.023	14.1	38.0	0.937
Fa-3c	59° 6.515′W	high traffic	*Dirinaria picta*	Microfoliose	192.5	495.6	26.8	3.6	1.7	0.018	13.9	36.2	0.949
Fa-4a	37° 19.295′S; 59° 6.471′W	Near factory, street, high traffic	*Parmotrema pilosum*	Foliose	174.7	483.5	26.4	3.9	1.8	0.018	15.1	36.7	0.979
CR-2	37° 19.613′S; 59° 6.527′W	Minor road, low traffic	*Punctelia hypoleucites*	Foliose	93.4	363.9	16.4	5.4	2.4	0.022	17.6	40.7	0.940
FR-1	37° 18.848′S; 59° 6.987′W	Near factory, street, moderate traffic	*Punctelia hypoleucites*	Foliose	103.2	369.8	14.8	5.0	3.4	0.025	14.4	38.0	0.945
FR-2a	37° 18.762′S;	Near factory, street,	*Punctelia hypoleucites*	Foliose	58.3	191.8	8.1	4.5	2.4	0.024	13.8	39.2	0.950
FR-2a″	59° 7.092′W	moderate traffic	*Punctelia hypoleucites*	Foliose	52.9	184.0	7.6	4.9	3.6	0.024	14.4	39.0	0.945
FR-2b			*Teloschistes chrysophthalmus*	Foliose	141.0	442.9	19.7	4.3	1.7	0.022	14.0	39.5	0.959
PR-1	37° 18.794′S; 59° 7.032′W	Factory, street, moderate traffic	*Punctelia subpraesignis*	Microfoliose	388.6	609.8	49.3	2.2	0.7	0.012	12.7	36.8	0.937
QU-1	37° 18.597′S; 59° 8.331′W	Street, low traffic	*Parmotrema pilosum*	Foliose	67.5	267.6	9.9	5.5	1.9	0.027	14.7	37.8	0.944
YR-1a	37° 19.482′S; 59° 8.354′W	Street, high traffic	*Parmotrema pilosum*	Foliose	101.8	363.2	13.4	5.0	4.6	0.027	13.2	37.3	0.906
YR-2b	37° 18.869′S; 59° 8.719′W	Near factory, street, high traffic	*Hyperphyscia aff coraloidea*	Microfoliose	184.0	413.6	24.7	3.1	2.5	0.017	13.4	37.7	0.945
YR-2c			*Dirinaria picta*	Microfoliose	118.4	310.5	16.8	3.7	2.8	0.019	14.2	38.3	0.947
LT-1b	37° 18.748′S;	Factory, street,	*Parmotrema pilosum*	Foliose	438.2	672.4	63.6	2.1	1.6	0.011	14.5	37.3	0.977
LT-1c	59° 8.869′W	high traffic	*Dirinaria applanata*	Microfoliose	499.7	849.4	76.3	2.3	0.8	0.011	15.3	37.5	0.968
Mu-1b	37° 18.788′S; 59° 8.717′W	Near factory, street, high traffic	*Parmotrema pilosum*	Foliose	160.3	491.7	23.8	4.3	2.2	0.021	14.8	39.2	0.938
CAS-1a	37° 21.880′S;	Control site (~5 km	*Parmotrema pilosum*	Foliose	26.6	175.4	4.2	9.3	1.6	0.042	15.7	37.3	0.876
CAS-1b	59° 6.057′W	from the town)	*Dirinaria picta*	Microfoliose	41.0	282.7	6.6	9.8	2.0	0.043	16.1	37.1	0.913
CAS-2	37° 21.861′S; 59° 6.064′W	Control site (~5 km from the town)	*Parmotrema pilosum*	Foliose	29.2	209.5	5.0	10.2	3.1	0.042	17.0	38.5	0.900
CAS-3a	37° 21.851′S;	Control site (~5 km	*Parmotrema pilosum*	Foliose	14.3	108.3	2.6	10.5	0.7	0.042	17.9	38.1	0.909
CAS-3b	59° 6.093′W	from the town)	*Flavorparmelia soredians*	Foliose	16.4	100.6	2.8	8.6	0.5	0.036	17.2	38.3	0.917
CAS-3c			*Punctelia hipoleucites*	Foliose	16.1	115.7	3.0	10.0	0.9	0.038	18.7	38.0	0.965
Pa-2a	37° 20.333′S;	Control site (~1 km	*Parmotrema pilosum*	Foliose	38.9	213.6	6.2	8.0	1.2	0.035	15.8	38.5	0.920
Pa-2b	59° 8.259′W	from the town)	*Punctelia hipoleucites*	Foliose	28.8	163.6	4.9	8.1	0.0	0.033	17.0	39.2	0.926
		Groups			Centroids from *K*-means clustering partitions								
		Group 1 ($n = 3$)			442.2	710.5	63.1	2.2	1.0	0.011	14.2	37.2	0.961
		Group 2 ($n = 9$)			156.5	439.5	22.1	4.0	1.7	0.020	14.1	37.6	0.954
		Group 3 ($n = 8$)			80.8	307.3	11.9	5.3	2.9	0.026	14.7	38.2	0.945
		Group 4 ($n = 9$)			33.1	212.1	5.4	9.3	1.4	0.039	16.8	37.8	0.916

Fig. 1. Map of sampling sites in Tandil (Argentina).

of remanent acquisition coercivity ($H_{1/2}$); the mean (and s.d.) Value was 54.3 (3.2) mt. The H_{cr} values varied also in a narrow range, between 34.6 and 40.7 mt, corresponding to magnetite-like minerals. There were no significant differences between H_{cr} values, at least to discriminate magnetic mineralogy between samples from rural, industrial and urban areas. Such a fact is also confirmed from the reproducibility of acquisition IRM curves (Fig. 2). In addition, it is possible to observe in Fig. 7 a linear trend between χ and SIRM ($R = 0.995$, the correlation is significant at the 0.01 level), which also supports the predominance of ferrimagnetic minerals.

On the other hand, it is possible to differentiate both areas, as well as different urban areas and areas close to industrial sites using magnetic-grain size-dependent parameters. The magnetic-grain size-distribution was estimated from the King's Plot (Fig. 3); as noted, magnetic-grain distribution varied widely; samples from control sites (CAS-1, CAS-2 and CAS-3) and relatively clean sites (Pa-2 and Ca-1) showed the finest fractions (<0.1 μm). In contrast, samples from polluted sites had coarser sizes, between 0.2 and 5 μm. This was also observed for other related parameters, such as, κ_{ARM}/κ and ARM/SIRM (Fig. 4, Table 1). Values of $\kappa_{ARM}/\kappa > 5$ correspond to submicron-sized magnetites (<0.1 μm) according to Peters and Dekkers (2003). Samples containing a higher fraction of finer magnetites (SD-PSD particles) yield higher ARM/SIRM values (Evans and Heller, 2003).

In Fig. 4, it is possible to observe three clear groups: sites with the finest magnetic grains are located on the upper part; the central part of this figure corresponds to samples affected by urban emissions (especially traffic-derived pollutants) and also industrial emissions (in particular, the coarsest fraction). The coarsest fraction is located in the lower part, corresponding to samples from sites close to the industrial sources (sites LT-1, PR-1, YR-2, Mu-1 and Fa). Most of these industries are relatively active metallurgical factories; currently, their surroundings are urbanised and people living there are adversely affected. A decade ago, Chaparro et al. (2002, 2006) studied soils close to the industrial area concluding that the pollution-influence of such factories; in this work, vegetal collectors (lichens) also revealed the load of pollutants in corresponding sites LT, YR, Mu, PR and Fa.

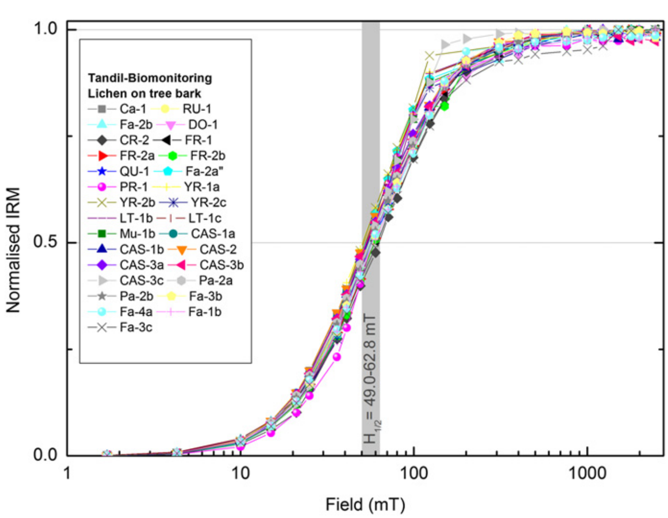

Fig. 2. Measurements of acquisition IRM for all ($n = 29$) lichen samples. A main ferrimagnetic phase with well-defined values of remanent acquisition coercivity ($H_{1/2}$) was observed.

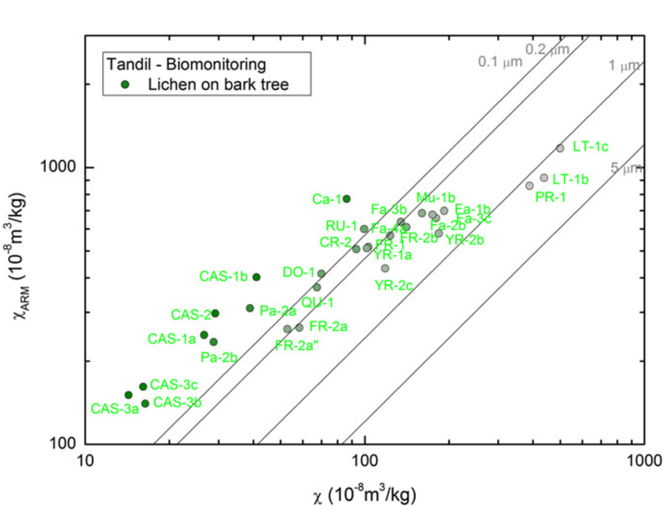

Fig. 3. King's plot (χ_{ARM} versus χ) for all lichen samples. Samples from polluted sites showed coarser magnetic grain sizes.

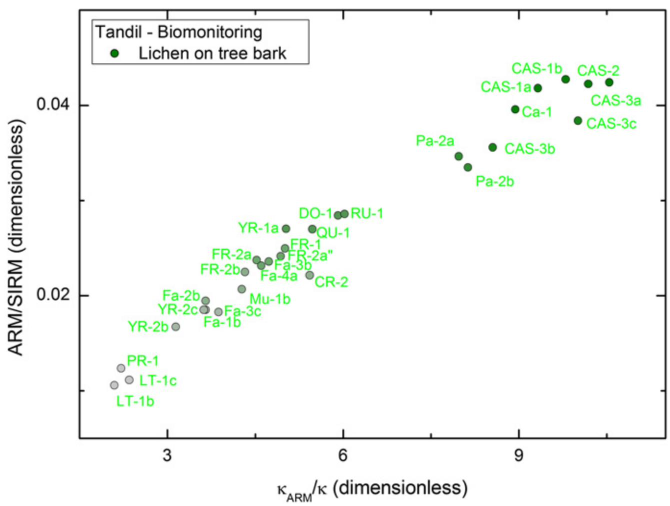

Fig. 4. Biplot ARM/SIRM vs. κ_{ARM}/κ for all lichen samples.

3.3. Magnetic comparison of different species

Most of the lichen samples seem to be adequate for magnetic monitoring. This can be appreciated from the magnetic properties of the most available species in the area: *P. Pilosum*, *Punctelia* spp. And *Dirinaria* spp. Comparable magnetic values at sites can be observed in Figs. 3 and 4; see for example, samples from site LT (1b *Punctelia* spp. And 1c *Dirinaria* spp.) And from site Pa (2a *P. Pilosum* and 2b *Punctelia* spp.). In addition, a comparison of lichen species in seven sampling sites can be seen in Fig. 5. Although different lichens (*Pa*, *D*, *P*, *F*, *H* and *T*; see Fig. 5) are compared, the magnetic concentration-dependent parameter (χ) and magnetic-grain size-dependent parameter (κ_{ARM}/κ) showed similar values at each site. As can be observed from this representation, different lichen species showed the same spatial pattern for both magnetic parameters. This magnetic fact allows the use of most of the studied lichens for magnetic monitoring. However, according to the occurrence of species in Tandil, lichens *P. Pilosum*, *Punctelia* spp. And *Dirinaria* spp. Are convenient choices for monitoring.

3.4. SEM-EDS

Observations by SEM from four lichen species (*D. Applanata*, *P. Pilosum*, *D. Picta* and *P. Hipoleucites*) and four contrasting sites (LT-1 and Fa-1 (industrial pollution), YR-1 (traffic-derived pollution) and CAS-3 (unpolluted)) are illustrated in Fig. 6. Such observations showed spherules and aggregates, agglomerates in a variety of shapes, and (sub) angular particles, as well as grain sizes in agreement with magnetic estimations (from <0.1 μm to 5 μm; see Fig. 3).

Samples from sites with industrial pollutant load (LT-1 and Fa-1) show a predominance of spherules ranging between 1 μm and 5 μm. The enlarged images show in detail the most abundant spherules (3–5 μm), as well as larger ones (13–15 μm). In addition to small (submicron-sized) aggregates on the surface of these spherules, agglomerates of micron-sized and smaller particles were also observed. Most of these spherules were iron oxides; the elemental composition of these particles is listed in Table 2, showing the dominance of C, O, Fe and Si. Other elements, such as N, K and Al seem to differentiate samples LT-1b, LT-1c and Fa-1b, respectively. The highest content of Fe from sample LT-1b (Table 2) is another distinctive characteristic. It is also worth mentioning that potentially toxic elements – i.e. Pb, Cu, Ni and Zn – were detected in low amounts for samples LT-1c and Fa-1b. The presence of these elements is in agreement with a previous work in soil by Chaparro et al. (2002, 2006) that showed higher contents of Pb and Zn (up to 223 and 173 mg/kg, respectively). Findings in these samples reveal the collection of pollutants from industrial origins accumulated in three different lichen species. Although *P. Pilosum* shows Fe-richer spherules than the *Dirinaria* spp., higher contents of C, as well as heavy metals were detected from the latter ones

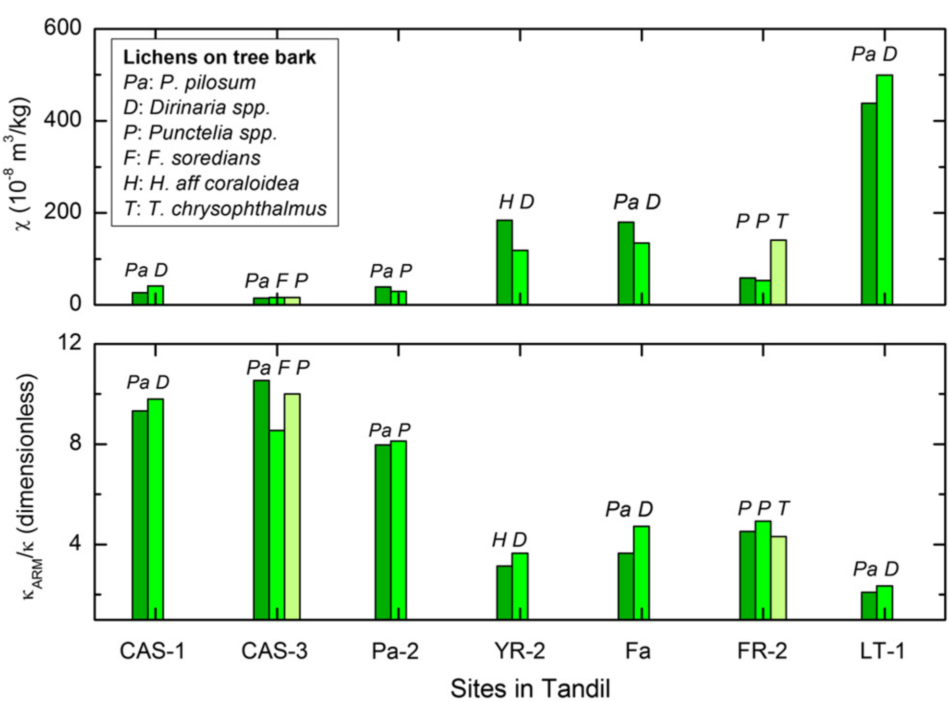

Fig. 5. Comparison of magnetic properties of lichen species in seven sampling sites.

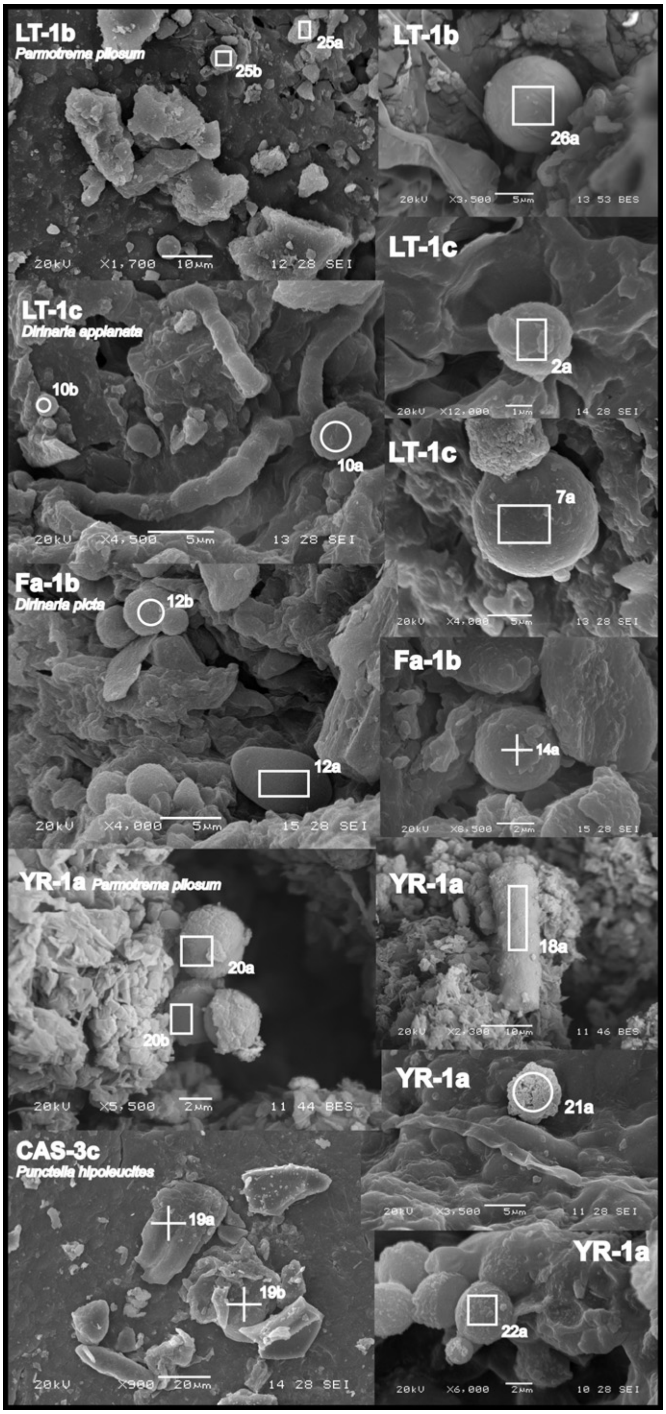

Fig. 6. SEM observations on selected samples: LT-1a (*P. Pilosum*), LT1c (*D. Applanata*), Fa-1b (*D. Picta*), YR-1a (*P. Pilosum*) and CAS-3c (*P. Hipoleucites*).

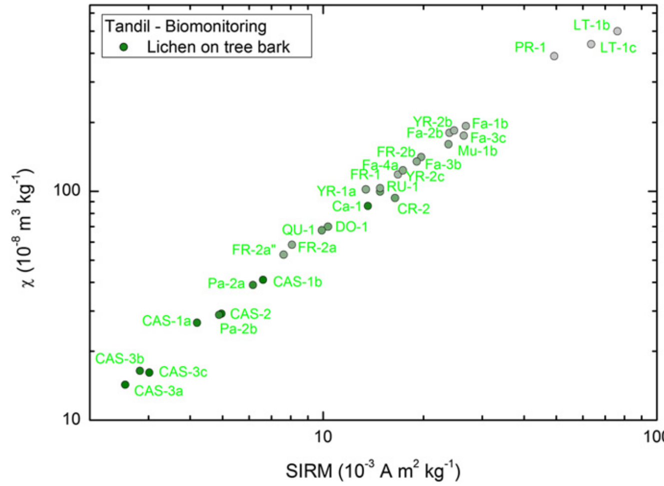

Fig. 7. Biplot of χ and SIRM for all lichen samples.

(Table 2). This fact may be related to the sensitivity of species, the lichen lifetime, and hence their accumulation period; *Dirinaria* spp. (microfoliose type) are more resistant to pollutants than the foliose type (*P. Pilosum*, Seaward, 1987). Nevertheless, future SEM-EDS studies on these autochthonous species from Tandil area should confirm this.

The SEM images obtained from samples YR-1a (high traffic urban site, 1.6–2.5 km from industrial sites) show finer grains (Fig. 6), and it is possible to observe spherules of 2–5 μm and finer ones, as well as smaller irregular particles probably from vehicles (wear particles). In addition, the spherules are different from the other ones, showing an irregular surface with aggregates of submicron-sized particles. Most of these particles come from traffic-derived pollution, the most important source in this urban

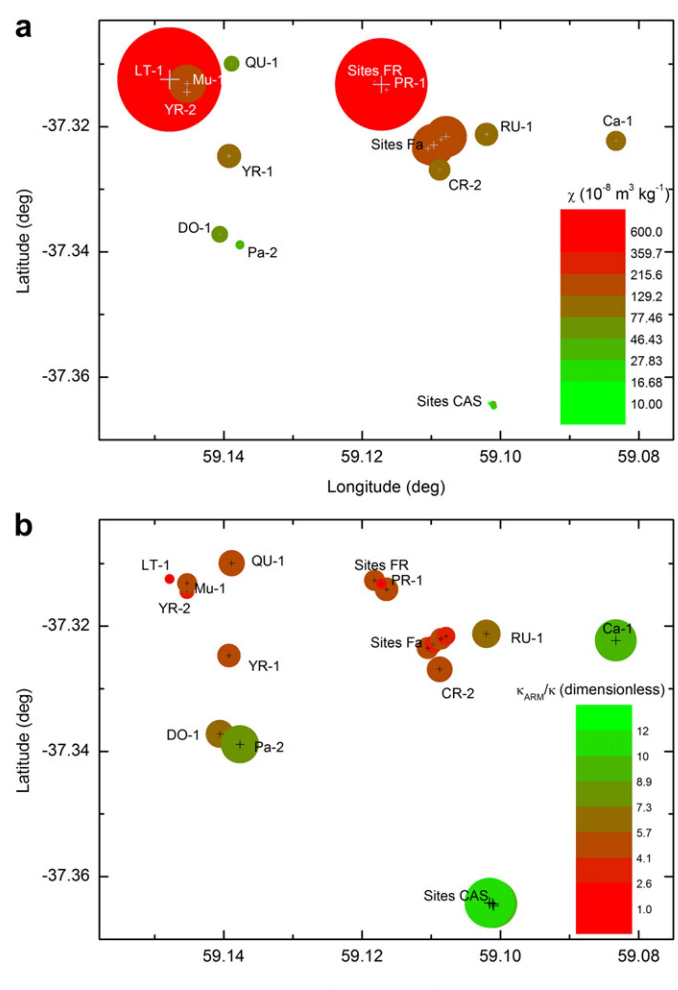

Fig. 8. (a) Mass-specific susceptibility and (b) κ_{ARM}/κ values in sampling sites from Tandil.

Table 2
Elemental composition by EDS analysis.

Element	Industrial sites										Urban sites					Rural sites	
	Sample LT-1b *Parmotrema pilosum*			Sample LT-1c *Dirinaria applanata*				Sample Fa-1b *Dirinaria picta*			Sample YR-1a *Parmotrema pilosum*					Sample CAS-3c *Punctelia hipoleucites*	
	25a Wt%	25b Wt%	26a Wt%	2a Wt%	7a Wt%	10a Wt%	10b Wt%	12a Wt%	12b Wt%	14a Wt%	18a Wt%	20a Wt%	20b Wt%	21a Wt%	22a Wt%	19a Wt%	19b Wt%
CK	20.67	30.02	9.58	40.23	26.46	43.69	40.74	49.36	52.83	17.93	45.75	45.48	39.16	43.40	51.44	49.00	35.16
NK	6.74	5.98	3.75	–	–	–	–	–	–	–	6.08	6.56	4.50	6.34	7.68	–	–
OK	27.11	23.23	23.79	5.17	11.56	11.79	19.19	14.46	12.39	25.03	18.18	8.54	5.40	14.93	15.49	6.31	10.17
NaK	0.17	0.14	0.13	–	–	0.24	0.24	0.10	0.04	0.73	0.12	0.00	0.00	0.16	0.04	–	0.26
MgK	0.26	0.14	0.12	0.13	0.21	0.23	0.42	0.48	0.25	0.69	0.26	0.06	0.09	0.10	0.17	–	0.45
AlK	0.85	0.36	0.35	0.13	1.10	0.87	2.06	1.26	0.80	5.47	1.41	0.18	0.18	0.67	0.45	0.15	2.19
SiK	4.36	0.89	0.73	0.74	3.44	2.38	4.82	3.04	1.96	16.99	3.46	0.46	0.61	2.64	1.30	0.42	6.54
PK	0.36	0.35	0.26	0.90	0.15	0.71	0.42	0.68	0.74	0.47	–	0.53	0.64	0.20	0.34	0.36	0.12
SK	0.08	0.56	0.00	0.96	0.13	0.86	0.29	0.37	0.50	–	0.57	0.77	0.92	0.08	1.01	–	–
PbM	–	–	–	–	0.42	–	1.00	–	–	–	–	–	–	–	–	–	–
ClK	–	–	–	–	0.10	0.11	0.04	–	–	–	–	–	–	–	–	0.48	0.08
KK	0.22	0.21	0.10	1.02	1.18	0.88	0.74	0.78	0.66	0.83	1.45	0.65	0.74	0.45	0.48	0.14	0.71
CaK	0.24	0.20	0.11	0.25	0.90	0.38	0.77	0.53	0.56	0.88	6.69	4.10	10.13	0.76	0.65	0.50	0.49
TiK	–	–	–	–	0.23	0.08	–	–	–	–	–	–	–	–	–	–	–
FeK	15.05	23.39	48.23	1.16	3.46	1.10	1.42	1.06	0.89	2.66	1.41	0.69	1.56	1.43	0.52	–	2.23
NiK	–	–	–	0.16	0.27	–	–	–	–	0.26	–	–	–	–	–	–	–
CuK	–	–	–	–	0.56	–	–	–	–	–	–	–	–	–	–	–	–
ZnK	–	–	–	–	0.53	–	–	–	–	0.12	–	–	–	–	–	–	–
AuL[a]	23.90	14.54	12.85	49.14	49.29	36.68	27.84	27.88	28.37	27.18	14.62	31.98	36.08	28.83	20.45	42.64	41.60

[a] For the specimen preparation, an Au/Pd coating was deposited.

site. According to Chaparro et al. (2010) sub and micron-sized particles are expected from the combustion of diesel- and gasoline-powered engines and the wear particles from brake materials. The elemental analysis shows the dominance of C, O, N and Ca, and to a lesser extent, Fe, S and Si (see Table 2). These elements, as well as others, were reported by Chaparro et al. (2010) as being from vehicle pollution sources from Argentina, and other authors have shown similar findings, e.g. Lin et al. (2005), Zhang et al. (2006), Mosleh et al. (2004), Vouitsis et al. (2009), Yao et al. (2009), and Qiao et al. (2011).

These lichen species seem to be good and appropriate bio-monitors of air pollutants released by metallurgical factories and the traffic of vehicles. This analysis confirms the presence of micron-sized Fe oxides and toxic elements on some observed lichens, i.e. *P. Pilosum* and *Dirinaria* spp.

On the other hand, the observations in samples from rural areas did not reveal the presence of characteristic spherules from industrial or traffic-derived origin. As illustrated in Fig. 6 (sample CAS-3c), most of these particles are probably of lithogenic origin; some of them are larger with well-defined edges, as well as particles of irregular morphology and agglomerates of different shapes and sizes. Their composition was determined in two large particles (sites 19a and 19b; see Fig. 6 and Table 2); both of them showed high concentrations of C, O and Si, and in lower proportion Al and Fe.

3.5. Magnetic concentration and monitoring

The magnetic concentration is another relevant property for this study, as noted in Figs. 3 and 8; there are not only differences (in order to group sites) in magnetic grain sizes, but also in magnetic concentration. The concentration-dependent magnetic parameters (i.e. χ, ARM and SIRM) showed a wide value range (14.3–500.0 $\times$ 10^{-8} m^3/kg, 100.6–894.4 $\times$ 10^{-6} A m^2/kg and 2.5–76.3 $\times$ 10^{-3} A m^2/kg, respectively; Table 1). From Fig. 7, control, urban and industrial sites showed important differences, and were well differentiated. Such differences (from the χ parameter) are interpreted as "magnetic enhancement" in agreement with previous studies (Chaparro et al., 2006), this characteristic discriminates control and polluted sites, as well as sites influenced by different pollution sources, i.e. Industrial and traffic-related pollutants.

As preliminary work in the construction of a map of magnetic monitoring, measurements of mass-specific magnetic susceptibility and κ_{ARM}/κ are presented in a bubble colour map (Fig. 8). In Fig. 8a, it is possible observe the magnetic concentration distribution of sampling sites in Tandil and the adverse influence of industrial sources (LT-1, PR-1 and sites Fa). In contrast, the lowest values correspond to control sites: a park in the urban area (Pa-2) and rural areas (sites CAS-1–3). The influence of factories can be appreciated from the decrease of magnetic concentration with distance. However, the same sites are also influenced by traffic-derived pollution; observe the magnetic changes from site LT-1 to Mu-1, YR-2, YR-1, DO-1 and Pa-2; as well as from sites Fa to CR-2, RU-1 and Ca-1. A similar pattern is observed from the grain-size-dependent parameter (Fig. 8b). In such a case, there is a decrease (increase of κ_{ARM}/κ values) in size of magnetic particles from the industrial pollution sources (LT, PR and Fa).

This qualitative discrimination is supported by multivariate statistical studies, which allows a classification of samples (and sites) from magnetic properties. Results from PCoordA, using the Gower's distance, allow searching in an exploratory way for similarities between individuals. For this analysis, the first two pcs accounted for 58% of the total variance (Fig. 9).

This qualitative information was used for the *K*-means clustering analysis (nine magnetic variables and the Gower's distance were also used; Table 1) in order to quantitatively confirm the observed groupings from the coordinate PCoordA plane. To validate the selection of groups, two numbers of groups $k = 3$ and $k = 4$ were studied. From the two possible options, the best is $k = 4$ where the within-cluster sum of squares is 4.75 ($k = 4$) and 5.20 ($k = 3$), respectively. In Table 1, centroids of each group by CA are shown.

Samples with industrial influence are grouped in group 1 ($n = 3$) and 2 ($n = 9$). The first group corresponds to the heavily polluted sites very close to metallurgical factories: LT-1 (Factory Metalúrgica Tandil) and PR-1 (Factory Tandilmat), which shows the highest values in magnetic concentration and coarser magnetic grains (see

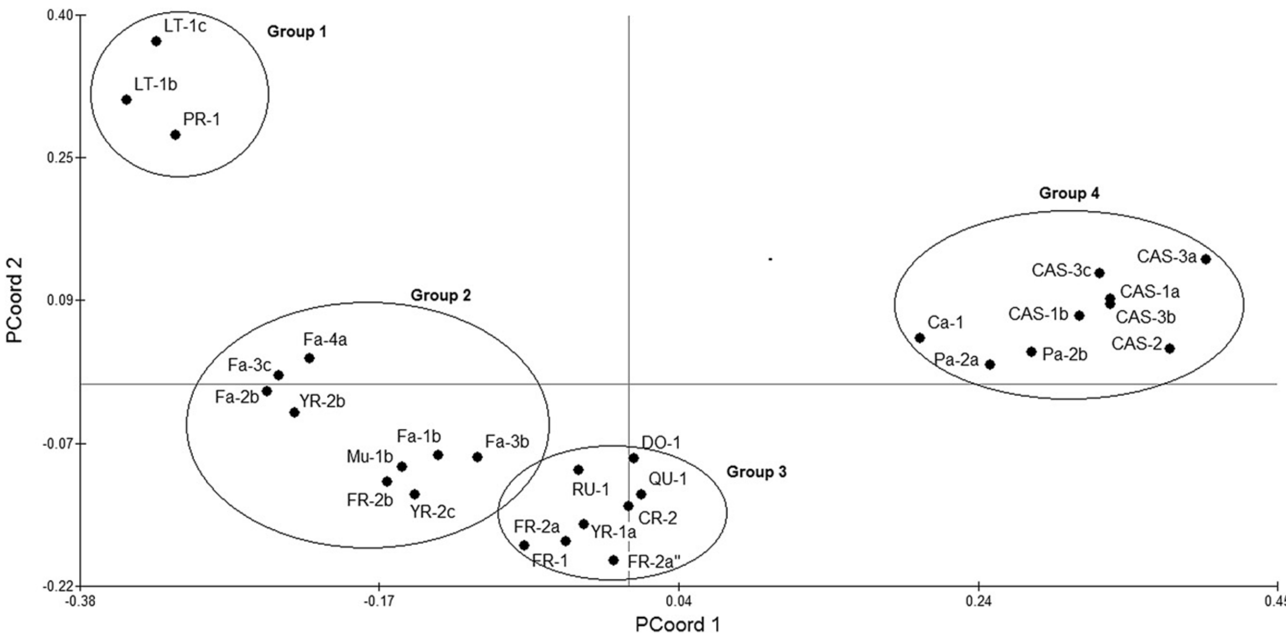

Fig. 9. Principal coordinate analysis (PCoordA). Individuals are identified and shown in the coordinate plane (PCoord 1 and PCoord 2). Groups 1–4 correspond to the classification by *K*-means clustering analysis.

values of centroids in Table 1). The second group comprises samples from another factory, samples Fa (Factory Ronicevi) and samples close to the above-mentioned factories (YR-2, Mu-1 and FR-2).

As seen in Fig. 9, samples influenced by vehicle-derived emission and mainly located in urban sites (YR-1, QU-1, RU-1 and DO-1) are represented in group 3 ($n = 8$). Although samples FR (FR-1 and FR-2) are near a factory, they are mixed with urban samples and are classified in this group.

Group 4 ($n = 9$) comprises samples from control sites, Pa-2, Ca-1 and sites CAS, showing the lowest magnetic concentration values, as well as highest values of grain-size-dependent parameters and hence finer particles.

4. Conclusions

The integrated rock-magnetic studies show the dominance of magnetite-like minerals for all lichen samples. The main magnetic carrier seems to be similar between control and urban sites, but magnetic grain size varies distinctively. For example, lichens from control sites accumulated the finest magnetic fractions (<0.1 μm) and, in contrast, lichens from urban and industrial sites accumulated coarser magnetic grains (0.2–5 μm). This conclusion is also observed by SEM observations in selected sites and species, showing the predominance of Fe-rich spherules with different grain sizes according to their origin, i.e. Industrial or traffic-derived sources.

The composition of spherules and other particles from industrial sites is C, O, Fe and Si; however, in lower proportion potentially toxic elements (Pb, Ni, Cu and Zn) were also detected. Although traffic-derived particles have similar elemental composition, additional elements (N, Ca and S) are present in considerable proportion.

The magnetic concentration varies widely between clean and polluted sites, up to 20-times (e.g. χ and SIRM). Such differences are interpreted as magnetic enhancement and are related to the influence of different pollution sources.

Sites with different pollution load were successfully classified by PCoordA and *K*-means clustering analysis; each group is especially characterised from concentration and grain-size-dependent magnetic parameters.

The comparison of lichens (living at same sites) using relevant magnetic parameters (magnetic concentration: χ, and magnetic grain size: κ_{ARM}/κ) and additional SEM-EDS analyses did not show significant differences, which supports the use of the available species in the study area. Most of the lichens appear suitable for air pollution monitoring, but according to the strategic distribution of species (i.e. Occurring more frequently) in Tandil, lichens *P. Pilosum*, *P. Hipoleucites* and *D. Picta* are convenient choices for future monitoring.

Acknowledgements

The authors wish to thank the UNCPBA, ANPCYT and CONICET for their financial support. They also thank Mr. P. Zubeldia (Tech. CICPBA) and Dr. M.A. Irurzun for their help. The authors also thank the three anonymous reviewers for their constructive comments that helped in improving the paper.

References

Adler, M.T., 1992. Clave de los géneros y las especies de Parmeliaceae (Lichenes Ascomycotina) de la Provincia de Buenos Aires (Argentina). Boletin Sociedad Argentina Botanica 28, 11–17.

Basile, A., Sorbo, S., Aprile, G., Conte, B., Castaldo Cobianchi, R., 2007. Comparison of the heavy metal bioaccumulation capacity of an epiphytic moss and an epiphytic lichen. Environmental Pollution 151 (2), 401–407.

Bermudez, G.M.A., Rodriguez, J.H., Pignata, M.L., 2009. Comparison of the air pollution biomonitoring ability of three Tillandsia species and the lichen *Ramalina celastri* in Argentina. Environmental Research 109, 6–14.

Calvelo, S., Liberatore, S., 2004. Applicability of in situ or transplanted lichens for assessment of atmospheric pollution in Patagonia, Argentina. Journal of Atmospheric Chemistry 49, 199–210.

Carreras, H.A., Pignata, M.L., 2002. Biomonitoring of heavy metals and air quality in Córdoba city, Argentina, using transplanted lichens. Environmental Pollution 177, 77–87.

Carreras, H.A., Wannaz, E.D., Perez, C.A., Pignata, M.L., 2005. The role of urban air pollutants on the performance of heavy metal accumulation in *Usnea amblyoclada*. Environmental Research 97, 50–57.

Chaparro, M.A.E., Gogorza, C.S., Lavat, A., Pazos, S., Sinito, A.M., 2002. Preliminary results of magnetic characterisation of different soils in Tandil region

(Argentina) affected by the pollution of metallurgical factory. European Journal Environmental and Engineering Geophysics 7, 35–58.
Chaparro, M.A.E., Gogorza, C.S.G., Chaparro, M.A.E., Irurzun, M.A., Sinito, A.M., 2006. Review of magnetism and pollution studies of various environments in Argentina. Earth Planets Space 58 (10), 1411–1422.
Chaparro, M.A.E., Chaparro, M.A.E., Marinelli, C., Sinito, A.M., 2008. Multivariate techniques as alternative statistical tools applied to magnetic proxies for pollution: cases of study from Argentina and Antarctica. Environmental Geology 54, 365–371.
Chaparro, M.A.E., Marié, D.C., Gogorza, C.S.G., Navas, A., Sinito, A.M., 2010. Magnetic studies and scanning electron microscopy—X-ray energy dispersive spectroscopy analyses of road sediments, soils, and vehicle-derived emissions. Studia Geophysica et Geodaetica 54 (4), 633–650.
Chaparro, M.A.E., Chaparro, M.A.E., Sinito, A.M., 2012. An interval fuzzy model for magnetic monitoring: estimation of a pollution index. Environmental Earth Sciences 66 (5), 1477–1485.
Cloquet, C., Demuynck, D., Signoret, J., Vanhaecke, F., 2009. Urban/Peri-Urban Aerosol Survey by determination of the concentration and isotopic composition of Pb collected by transplanted lichen *Hypogymnia physodes*. Environmental Science & Technology 43, 623–629.
Evans, M.E., Heller, F., 2003. Environmental Magnetism. Principles and Applications of Enviromagnetics. Academic Press. An imprint of Elsevier Science, USA, 299 pp.
Fabian, K., Reimann, C., mcenroe, S.A., Willemoes-Wissing, B., 2011. Magnetic properties of terrestrial moss (*Hylocomium splendens*) along a north–south profile crossing the city of Oslo, Norway. Science of the Total Environment 409, 2252–2260.
Flanders, P.J., 1994. Collection, measurement, and analysis of airborne magnetic particulates from pollution in the environment. Journal of Applied Physics 75 (10), 5931–5936.
Gautam, P., Blahab, U., Appel, E., 2005. Magnetic susceptibility of dust-loaded leaves as a proxy of traffic-related heavy metal pollution in Kathmandu city, Nepal. Atmospheric Environment 39, 2201–2211.
Getty, S.R., Gutzler, D.S., Asmerom, Y., Shearer, C.K., Free, S.J., 1999. Chemical signals of epiphytic lichens in southwestern North America; natural versus man-made sources for airborne particulates. Atmospheric Environment 33, 5095–5104.
Gower, J.C., 1966. Some distance properties of latent root and vector methods used in multivariate analysis. Biometrika 53, 325–338.
Gower, J.C., 1987. Introduction to ordination techniques. In: Legendre, P., Legendre, L. (Eds.), Development in Numerical Ecology. Springer-Verlag, Berlin, pp. 3–64.
Guerra, M.B.B., Amarasiriwardena, D., Schaefer, C.E.G.R., Pereira, C.D., Spielmann, A.A., Nobrega, J.A., Pereira-Filho, E.R., 2011. Biomonitoring of lead in Antarctic lichens using laser ablation inductively coupled plasma mass spectrometry. Journal of Analytical Atomic Spectrometry 26, 2238–2246.
Hanesch, M., Scholger, R., Rey, D., 2003. Mapping dust distribution around an industrial site by measuring magnetic parameters of tree leaves. Atmospheric Environment 37, 5125–5133.
Hawksworth, D.L., Rose, F., 1970. Qualitative scale for estimating sulphur dioxide air pollution in England and Wales using epiphytic lichens. Nature 227, 145–148.
Hazarika, N., Daimari, R., Nayaka, S., Hoque, R., 2011. What do epiphytic lichens of Guwahati city indicate? Current Science 101 (07), 824.
infostat, 2009. infostat versión 2009. Grupo infostat, FCA, Universidad Nacional de Córdoba, Argentina.
Jasan, R.C., Verburg, T.G., Wolterbeek, H.Th., Plá,, R.R., Pignata, M.L., 2004. On the use of the lichen *Ramalina celastri* (Spreng.) Krog & Swinsc as an indicator of atmospheric pollution in the Province of Córdoba (Argentina), considering both lichen physiological parameters and element concentrations. Journal of Radioanalytical and Nuclear Chemistry 259, 93–97.
Jordanova, N.V., Jordanova, D.V., Veneva, L., Andorova, K., Petrovský, E., 2003. Magnetic response of soils and vegetation to heavy metal pollution — a case of study. Environmental Science & Technology 37, 4417–4424.
Jordanova, D., Petrov, P., Hoffmann, V., Gocht, T., Panaiotu, C., Tsacheva, T., Jordanova, N., 2010. Magnetic signature of different vegetation species in polluted environment. Studia Geophysica et Geodaetica 54, 417–442.
King, J., Banerjee, S.K., Marvin, J., Özdemir, Ö., 1982. A comparison of different magnetic methods for determining the relative grain size of magnetite in natural materials: some results from lake sediments. Earth and Planetary Science Letters 59, 404–419.
Lavornia, J.M., 2009. Las comunidades de líquenes de Tandil (Buenos Aires), como bioindicadoras de la calidad del aire (The communities of Lichens from Tandil (Buenos Aires), as Bioindicators of Air Quality). Unpublished thesis of Bachelor's degree in Environmental Management and Diagnosis, FCH. UNCPBA.
Lehndorff, E., Urbat, M., Schwark, L., 2006. Accumulation histories of magnetic particles on pine needles as function of air quality. Atmospheric Environment 40, 7082–7096.
Lin, C.-C., Chen, S.-J., Huang, K.L., 2005. Characteristics of metals in nano/ultrafine/fine/coarse particles collected beside a heavily trafficked road. Environmental Science & Technology 39, 8113–8122.
Maher, B.A., Moore, C., Matzka, J., 2008. Spatial variation in vehicle-derived metal pollution identified by magnetic and elemental analysis of roadside tree leaves. Atmospheric Environment 42, 364–373.
Matzka, J., Maher, B.A., 1999. Magnetic biomonitoring of roadside tree leaves: identification of spatial and temporal variations in vehicle-derived particulates. Atmospheric Environment 33, 4565–4569.
Mitchell, R., Maher, B.A., Kinnersley, R., 2010. Rates of particulate pollution deposition onto leaf surfaces: temporal and inter-species magnetic analyses. Environmental Pollution 158, 1472–1478.
Moreno, E., Sagnotti, L., Dinares-Turell, J., Winkler, A., Cascella, A., 2003. Biomonitoring of traffic air pollution in Rome using magnetic properties of tree leaves. Atmospheric Environment 37, 2967–2977.
Mosleh, M., Blau, P.J., Dumitrescu, D., 2004. Characteristics and morphology of wear particles from laboratory testing of disk brake materials. Wear 256, 1128–1134.
Peters, C., Dekkers, M., 2003. Selected room temperature magnetic parameters as a function of mineralogy, concentration and grain size. Physics and Chemistry of the Earth 28, 659–667.
Petrovský, E., Ellwood, B., 1999. Magnetic monitoring of air, land and water pollution. In: Maher, B.A., Thompson, R. (Eds.), Quaternary Climates, Environment and Magnetism. Cambridge University Press, pp. 279–322.
Pfeiffer, H.N., Barclay-Estrup, P., 1992. The use of a single lichen species, *Hypogimnia physodes*, as an indicator of air quality in northwestern Ontario. Bryologist 95, 3–41.
Pignata, M.L., González, C.M., Wannaz, E.D., Carreras, H.A., Gudiño, G.L., Martinez, M.S., 2004. Biomonitoring of air quality employing in situ *Ramalina celastri* in Argentina. International Journal of Environment and Pollution 22, 409–429.
Qiao, Q., Zhang, C., Huang, B., Piper, J.D.A., 2011. Evaluating the environmental quality impact of the 2008 Beijing Olympic Games: magnetic monitoring of street dust in Beijing Olympic Park. Geophysical Journal International 187, 1222–1236.
Salo, H., Bucko, M.S., Vaahtovuo, E., Limo, J., Mäkinen, J., Pesonen, L.J., 2012. Biomonitoring of air pollution in SW Finland by magnetic and chemical measurements of moss bags and lichens. Journal of Geochemical Exploration 115, 69–81.
Scerbo, R., Ristori, T., Possenti, L., Lampugnani, L., Barale, R., Barghigiani, C., 2002. Lichen (*Xanthoria parietina*) biomonitoring of trace element contamination and air quality assessment in Pisa Province (Tuscany, Italy). Science of the Total Environment 286, 27–40.
Scutari, N., 1992. Estudios sobre *Pyxinaceae foliosas* (Lecanorales, Ascomycotina) de la Argentina, IV: claves de los géneros y las especies de la provincia de Buenos Aires. Boletin Sociedad Argentina Botanica 28, 169–173.
Seaward, M.R.D., 1987. Effects of quantitative and qualitative changes in air pollution on the ecological and geographical performance of lichens. In: Hutchinson, T.C., Meema, K.M. (Eds.), Effects of Atmospheric Pollutants on Forests, Wetlands and Agricultural Ecosystems. 133: NATO ASI Series, vol. G16. Springer-Verlag, Berlin-Heidelberg.
Sutton, M.A., Pitcairn, C.E.R., Leith, I.D., van Dijk, N., Tang, Y.S., Skiba, U., Smart, S., Mitchell, R., Wolseley, P., James, P., Purvis, W., Fowler, D., 2004. Bioindicator and Biomonitoring Methods for Assessing the Effects of Atmospheric Nitrogen on Statutory Nature Conservation Sites. In: Sutton, M.A., Pitcairn, C.E.R., Whitfield, C.P. (Eds.), JNCC Report No. 356, Peterborough.
Thompson, R., Oldfield, F., 1986. Environmental Magnetism. Allen & Unwin (Publishers) Ltd., 225 pp.
Vouitsis, E., Ntziachristos, L., Pistikopoulos, P., Samaras, Z., Chrysikou, L., Samara, C., Papadimitriou, C., Samaras, P., Sakellaropoulos, G., 2009. An investigation on the physical, chemical and ecotoxicological characteristics of particulate matter emitted from light-duty vehicles. Environmental Pollution 157, 2320–2327.
Wannaz, E.D., Carreras, H.A., Pérez, C.A., Pignata, M.L., 2006. Assessment of heavy metal accumulation in two species of Tillandsia in relation to atmospheric emission sources in Argentina. Science of the Total Environment 361, 267–278.
Yao, Q., Li, S.-Q., Xu, H.-W., Zhuo, J.-K., Song, Q., 2009. Studies on formation and control of combustion particulate matter in China: a review. Energy 34, 1296–1309.
Zhang, C.X., Huang, B.C., Li, Z.Y., Liu, H., 2006. Magnetic properties of highroad-side pine tree leaves in Beijing and their environmental significance. Chinese Science Bulletin 51 (24), 3041–3052.
Zhang, C.X., Huang, B.C., Piper, J.D.A., Luo, R.S., 2008. Biomonitoring of atmospheric particulate matter using magnetic properties of *Salix matsudana* tree ring cores. Science of the Total Environment 393, 177–190.
Zhang, C.X., Quiao, Q., Appel, E., Huang, B.C., 2012. Discriminating sources of anthropogenic heavy metals in urban street dusts using magnetic and chemical methods. Journal of Geochemical Exploration 119–120, 60–75.